Acta Cryst. (1983). B39, 217–226

Structure and Crystal Chemistry of Mixed-Valence Ternary Platinum Oxides: $MnPt_3O_6$, $CoPt_3O_6$, $ZnPt_3O_6$, $MgPt_3O_6$, and $NiPt_3O_6$

BY K. B. SCHWARTZ,* J. B. PARISE AND C. T. PREWITT

Department of Earth and Space Sciences, State University of New York at Stony Brook, Stony Brook, New York 11794, *USA*

AND R. D. SHANNON

Central Research and Development Department,† E.I. du Pont de Nemours and Company, Wilmington, Delaware 19898, *USA*

(*Received* 13 *May* 1982; *accepted* 26 *October* 1982)

Abstract

The structures of the mixed-valence series of MPt_3O_6 compounds with approximate compositions $MnPt_3O_6$, $CoPt_3O_6$, $ZnPt_3O_6$, $MgPt_3O_6$, and $NiPt_3O_6$ have been refined from neutron powder diffraction experiments. The first four were isostructural with the prototype *C*-centered $CdPt_3O_6$, containing a rigid framework of planar PtO_4 and octahedral PtO_6 groups and a distorted eight-coordinated counterion site consisting of two interpenetrating rectangular planes. Further distortions of the counterion site in $NiPt_3O_6$ caused a change in symmetry to a primitive lattice, thereby distinguishing its structure from those of the other known MPt_3O_6 compositions. The presence of some cation disorder and vacancies was established from refinements of site occupancies constrained by known values of counterion content determined by independent chemical analysis. The $MnPt_3O_6$ structure was refined in *Cmmm* with $Z = 2$ [$a = 7{\cdot}152\,(1)$, $b = 10{\cdot}045\,(1)$, $c = 3{\cdot}1476\,(3)$ Å] by the Rietveld profile technique to a final $R_{wP} = 0{\cdot}171$ for data collected at $\lambda = 1{\cdot}30$ Å. The $CoPt_3O_6$, $ZnPt_3O_6$, and $MgPt_3O_6$ structures were also refined in *Cmmm* using integrated intensities for data collected at $\lambda = 2{\cdot}46$ Å to $R_w = 0{\cdot}041$, 0·046, and 0·076, respectively. The $NiPt_3O_6$ structure was refined in *Pbam* with $Z = 2$ [$a = 7{\cdot}123\,(1)$, $b = 9{\cdot}933\,(1)$, $c = 3{\cdot}100\,(1)$ Å] from similar data to a $R_w = 0{\cdot}050$. The structure is characterized by the presence of columnar stacks of planar PtO_4 groups, metal–metal distances along the *c* axis of 3·10 to 3·14 Å, and examples of partial oxidation of planar platinum chains caused by non-stoichiometry and multiple counterion occupancy, consistent with high conductivity resulting from one-dimensional metal–metal interactions.

1. Introduction

Orthorhombic platinum–metal oxides of the type MPt_3O_6 are of technological interest due to the catalytic properties these compounds exhibit. A variety of compositions have been reported, with counterion M = Mn, Fe, Co, Ni, Cu, Zn, Mg, Cd, Hg, and Ca (Muller & Roy, 1969; Hoekstra, Siegel & Gallagher, 1971; Shannon, 1972; Carcia, Shannon & Staikos, 1981). MPt_3O_6 compounds have been used for hydrogenation of ethylene (Shannon, 1972). They also exhibit high activity as catalysts in electrochemical processes for the reduction of oxygen in acid electrolytes, and can therefore be used as the cathode in acid-electrolyte fuel cells (Carcia, Shannon & Staikos, 1981).

The structure of MPt_3O_6 is known from a single-crystal X-ray study of $CdPt_3O_6$ (Shannon, 1972; Prewitt, Schwartz & Shannon, 1983). The orthorhombic structure has unit-cell dimensions $a = 7{\cdot}214\,(1)$, $b = 10{\cdot}190\,(1)$, and $c = 3{\cdot}1650\,(2)$ Å; in *Cmmm* with $Z = 2$. The ideal stoichiometric structure (Fig. 1) has formally divalent platinum in a four-coordinated planar site, octahedrally coordinated Pt^{4+}, and eight-coordinated Cd^{2+} cations. It has previously been assumed that orthorhombic MPt_3O_6 compounds with M = Mn, Co, Zn, Mg, and Ni have this same structure (Shannon, 1972), based on similarities of their X-ray powder diffraction patterns, but $CuPt_3O_6$ has a different structure (Muller & Roy, 1969; Shannon, 1972). However, structural investigations of platinum–metal oxides with X-ray powder diffraction techniques provide limited information concerning O atoms and counterions due to the overwhelming contribution to the scattering from Pt (Schwartz, Prewitt, Shannon, Corliss, Hastings & Chamberland, 1982).

The family of MPt_3O_6 compounds is also of interest for other reasons. The eightfold coordination of the first-row transition metals, although known for Mn^{2+}

* Current address: Lawrence Livermore National Laboratory, PO Box 808, L-396, Livermore, CA 94550, USA.

† Contribution No. 3048.

0567-7408/83/020217-10$01.50

(*e.g.* the naturally occurring mineral spessartine), is rare for Co {*e.g.* $[Co(NO_3)_4]^{2-}$ groups (Bergman & Cotton, 1966) and $(Co_xNa_y)Pt_3O_4$ (Schwartz, Parise, Prewitt & Shannon, 1982)} and Zn {$[Zn(NO_3)_4]^{2-}$ groups (Bellito, Gastaldi & Tomlinson, 1976)} and unknown for Ni. The MPt_3O_6 structure is also a mixed-valence system in which metal–metal interactions may be enhanced by non-stoichiometry. $CoPt_3O_6$, and $Mn_{1+x}Pt_{3-x}O_6$ ($x \sim 0{\cdot}2$) are highly conducting semiconductors (Schwartz, Gillson & Shannon, 1982) with room-temperature conductivities on the order of 10^3–10^4 Ω^{-1} m^{-1} and activation energies of $<0{\cdot}1$ eV (1 eV $\equiv$ $1{\cdot}60 \times 10^{-19}$ J). One-dimensional metal–metal interactions parallel to the *c* axis between square-planar platinum cations have been suggested by Cahen, Ibers & Wagner (1974) for $CdPt_3O_6$, and may be enhanced by chemical non-stoichiometry (Schwartz & Parise, 1982).

This paper describes the structure and crystal chemistry of platinum–metal oxides with the approximate compositions: $MnPt_3O_6$, $CoPt_3O_6$, $ZnPt_3O_6$, $MgPt_3O_6$, and $NiPt_3O_6$. As in previous studies of ternary platinum oxides, structure refinements are performed with neutron powder diffraction data (Schwartz, Prewitt, Shannon, Corliss, Hastings & Chamberland, 1982; Schwartz, Parise, Prewitt & Shannon, 1982) to investigate more fully the positions and occupancies of the light metal counterions and oxygen anions in the structure. Constraints provided by determinations of counterion content by atomic absorption analysis enable cation distributions to be ascertained, and deviations from stoichiometry, first suggested by Shannon (1972), to be examined. This information provides more insight into the relationships between the structure, crystal chemistry, and physical properties of these unique and interesting MPt_3O_6 compounds.

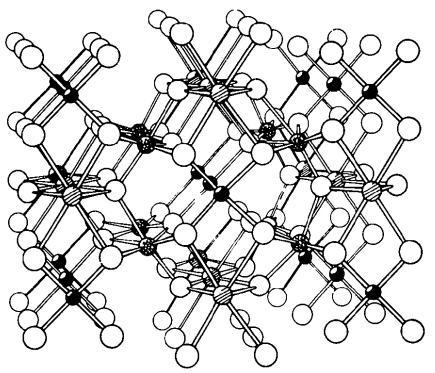

Fig. 1. The MPt_3O_6 structure, space group *Cmmm*. The black circles represent the planar site, the cross-hatched circles the octahedral site, and the single-hatched circles the eight-coordinated site. The white circles represent O.

2. Experimental

Polycrystalline $MnPt_3O_6$, $CoPt_3O_6$, $ZnPt_3O_6$, and $MgPt_3O_6$ were synthesized by solid-state reaction of α-PtO_2 obtained from Engelhard Industries with reagent-grade MnO, CoO, ZnO, and $Mg(OH)_2$, respectively, in a molar ratio of 2·5:1·0. $NiPt_3O_6$ was synthesized by an identical reaction using α-PtO_2 and NiO in a molar ratio of 2:1. In all cases, 15–17 g mixtures were ground thoroughly, pressed into pellets in an 8 mm die at 1500 lbs (680 kg) and sealed in thin-walled platinum tubes with a diameter of 9·5 mm. These sealed capsules were heated to 1123 K at 0·3 GPa for 24 h in an internally heated reactor using argon gas as the pressure medium. The resulting fine-grained black powders were boiled twice in *aqua regia* and washed thoroughly with distilled water to dissolve unreacted MnO, CoO, ZnO, $Mg(OH)_2$, or NiO. Attempts to prepare samples with stoichiometric mixtures of starting materials tended to give impurities of β-PtO_2.

Unit-cell dimensions were determined for these orthorhombic phases by least-squares refinement of line positions from X-ray powder diffraction patterns obtained with a Guinier–Hägg focusing camera having a radius of 40 mm. Monochromatic Cu $K\alpha_1$ radiation (λ = 1·5405 Å) and an internal standard of Si (a = 5·4305 Å) were used. Line positions on the film were determined to ± 5 μm with a David Mann film reader. The values obtained are given in Table 1. The patterns were single phases except in the case of $MgPt_3O_6$, for which very weak reflections corresponding to β-PtO_2 were detected.

Counterion contents were determined by duplicate atomic absorption analysis for all samples except $MnPt_3O_6$, where only a single analysis was performed. This chemical information was used to constrain occupancy parameters during the refinement procedure. The values obtained (in wt%) were: 7·73 for Mn in $MnPt_3O_6$, 8·73 for Co in $CoPt_3O_6$, 8·38 for Zn in $ZnPt_3O_6$, 3·0 for Mg in $MgPt_3O_6$, and 9·30 for Ni in $NiPt_3O_6$. Analyses performed in duplicate were reproducible to 1% with the exception of that for Mg, which was reproducible to within only 7% of the mean analyzed value. These analyses, when compared with ideal compositions for MPt_3O_6 compounds, indicated excess Mn, Co, and Ni and deficient Mg and Zn, suggesting non-stoichiometry which was examined in more detail during the refinement process.

Table 1. *Unit-cell dimensions for* MPt_3O_6

	a	*b*	*c*
$MnPt_3O_6$	7·152 (1) Å	10·045 (1) Å	3·1476 (3) Å
$CoPt_3O_6$	7·085 (2)	9·941 (3)	3·1427 (8)
$ZnPt_3O_6$	7·133 (3)	9·956 (4)	3·138 (1)
$MgPt_3O_6$	7·122 (1)	9·940 (1)	3·141 (1)
$NiPt_3O_6$	7·123 (1)	9·933 (1)	3·100 (1)

Neutron powder diffraction experiments were performed at room temperature at the High-Flux-Beam Reactor at Brookhaven National Laboratory. The powder sample of $MnPt_3O_6$ was placed in a cylindrical vanadium can 4·76 mm in diameter. A germanium monochromator in the (111) setting and a pyrolytic-graphite analyzer in the (004) setting were used and data for $MnPt_3O_6$ were collected at a wavelength of 1·30 Å over the 2θ range 6·00 to 96·50° with a 2θ step width of 0·05° and a counting time of 92 s/step. The powder samples of $CoPt_3O_6$, $ZnPt_3O_6$, $MgPt_3O_6$, and $NiPt_3O_6$ were pressed into cylindrical pellets approximately 10 mm in diameter and 20 mm in length and placed in the neutron beam with no holder. The data for $CoPt_3O_6$, $ZnPt_3O_6$, $MgPt_3O_6$, and $NiPt_3O_6$ were collected at a wavelength of 2·46 Å with a pyrolytic-graphite monochromator in the (002) setting and a pyrolytic-graphite analyzer in the (004) setting over the 2θ ranges: 10·0 to 138·9°, 22·0 to 133·8°, 12·0 to 136·9°, and 12·0 to 136·0°, respectively, with a 2θ step width of 0·1° and a counting time of 50 s/step.

Refinement of the structure of $MnPt_3O_6$ was performed by use of the method of profile analysis with the program *PROFILE* written by Rietveld (1969*a*,*b*) and modified by Hewat (1973). Structure refinements for $CoPt_3O_6$, $ZnPt_3O_6$, $MgPt_3O_6$, and $NiPt_3O_6$ were carried out using integrated intensities with the program *POWLS* (Will, 1979). Both programs have been used successfully with neutron powder diffraction data for refinement of the structures of ternary platinum oxides of the type $M_xPt_3O_4$, where M = Na, Co, Li (Schwartz, Prewitt, Shannon, Corliss, Hastings & Chamberland, 1982; Schwartz, Parise, Prewitt & Shannon, 1982). The neutron scattering amplitudes used (in fm) were: b(Mn) = −3·7, b(Co) = 2·80, b(Zn) = 5·7, b(Mg) = 5·38, b(Ni) = 10·3, b(Pt) = 9·5, and b(O) = 5·800 (Bacon, 1978; Koester, 1977).

Discrepancy factors for the structure refinement of $MnPt_3O_6$ using *PROFILE* are defined as $R_I = \sum|I_{obs} - I_{calc}|/\sum I_{obs}$ for integrated intensities determined by the approximation given by Rietveld (1969*a*,*b*) and $R_{wP} = [\sum w(Y_{obs} - Y_{calc})^2/\sum w(Y_{obs})^2]^{1/2}$ for weighted point-by-point intensities. The expected discrepancy factor $R_E = [(N - P + C)/\sum w(Y_{obs})^2]^{1/2}$. For structure refinements of $CoPt_3O_6$, $ZnPt_3O_6$, $MgPt_3O_6$, and $NiPt_3O_6$ using *POWLS*, the discrepancy factors are $R = \sum|I_{obs} - I_{calc}|/\sum I_{obs}$ and $R_w = [\sum w(I_{obs} - I_{calc})^2/\sum w(I_{obs})^2]^{1/2}$. The goodness-of-fit $\chi^2 = [\sum w(I_{obs} - I_{calc})^2/(N - P + C)]^{1/2}$. The expression $(N - P + C)$ represents the number of degrees of freedom.

3. Results

3.1. *Structure refinement of* $MnPt_3O_6$

The neutron powder diffraction pattern for $MnPt_3O_6$ collected at 1·30 Å was consistent with the expectations that this composition is isostructural with $CdPt_3O_6$. All reflections were indexed on an orthorhombic unit cell with systematic absences hkl: $h + k \neq 2n$, indicating a C-centered lattice. Refinement of the structure in *Cmmm* with these data was successfully achieved by use of *PROFILE*. The data comprised 119 independent reflections.

The structure refinement for $MnPt_3O_6$ included the standard *PROFILE* parameters: scale factor, half-width parameters U, V, and W, zero-point of the pattern Z, and unit-cell parameters a, b, and c; and three positional parameters: y for the O atom O(1) at site 4(j), and x and y for the O atom O(2) at site 8(p). The metal positions are fixed with the eight-coordinated cation at site 2(b), the octahedrally coordinated cation at site 4(f), and the planar cation at site 2(a). Throughout the refinement procedure, irrespective of the various models for occupancy and thermal motion which were examined, the refined values of these positional parameters never varied by greater than one standard deviation from the final values, given in column (I) of Table 2.*

Initially, an overall temperature factor was used. Ideal stoichiometry with no cation disorder was assumed and the resulting value of R_{wP} was 0·179. A structure refinement with individual isotropic tem-

* Lists of intensities for the five compounds have been deposited with the British Library Lending Division as Supplementary Publication No. SUP 38221 (4 pp.). Copies may be obtained through The Executive Secretary, International Union of Crystallography, 5 Abbey Square, Chester CH1 2HU, England.

Table 2. *Structure refinements for* MPt_3O_6 *compounds (orthorhombic, Cmmm;* M = Mn, Co, Zn, Mg)

		x	y	z
^{VIII}M	2(b)	½	0	0
^{IV}Pt(1)	2(a)	0	0	0
^{VI}Pt(2)	4(f)	¼	¼	½
O(1)	4(j)	0	y	½
O(2)	8(p)	x	y	0

	(I) Mn	(II) Co	(III) Zn	(IV) Mg
Occupancy:* ^{VIII}M	0·88 (1)†	0·92 (2)	0·95	1·0
Occupancy: ^{IV}Pt	1·0	1·0	1·0	1·0
Occupancy: ^{VI}Pt	1·87 (1)	1·86 (2)	2·0	2·0
Occupancy: ^{VI}M	0.13 (1)	0·14 (2)	—	—
Occupancy: O(1)	2·0	2·0	2·0	2·0
Occupancy: O(2)	4·0	4·0	4·0	4·0
y: O(1)	0·344 (1)	0·349 (1)	0·349 (2)	0·348 (2)
x: O(2)	0·210 (1)	0·212 (1)	0·211 (1)	0·210 (1)
y: O(2)	0·128 (1)	0·128 (1)	0·124 (1)	0·126 (1)
B (overall)‡	0·45 (3)	0·4 (2)	−0·2 (3)	−0·2 (2)
R_I	0·039	χ^2 1·01	1·44	2·07
R_{wP}	0·171	R 0·025	0·033	0·053
R_E	0·153	R_w 0·041	0·046	0·076

* Occupancies given in atoms per formula unit (see text).
† Errors in parentheses.
‡ Overall isotropic temperature factor (Å²).

perature factors for each atomic species which corresponds to two additional parameters produced a decrease in R_{wP} to 0·177. This was judged insignificant, and an overall temperature factor was used for all ensuing refinements.

At this stage, the possibility of both cation disorder and vacancies was considered by independently refining various combinations of the site scattering lengths with no constraints on overall chemical composition. These refinements indicated that the eightfold and sixfold sites were significantly deficient in scattering power relative to that expected for a stoichiometric composition, while the scattering lengths of the planar Pt and two O sites indicated no deviation from stoichiometric composition. The independent chemical analysis for the Mn content was then introduced, together with one additional parameter, to allow for Mn disorder between the eightfold and sixfold sites. The refinement was carried out on this basis, with the Mn content now constrained to the chemical analysis. This corresponded to the general formula:

$$^{VIII}\{Mn_{1-x}\square_x\}^{IV}[Pt]^{VI}(Pt_{1\cdot97-0\cdot77x}Mn_{0\cdot77x+0\cdot03})O_6$$

where x was now a variable parameter.

The final refinement, performed according to the constraints outlined above, with the one additional parameter which models cation disorder and vacancies, gives a value of R_{wP} of 0·171, with $R_E = 0\cdot153$ and $R_I = 0\cdot039$. It is once more to be emphasized that the positional parameters in all these refinements never varied by more than one estimated standard deviation from the final values given in column (I) of Table 2. The final refined values of the occupancy parameter x correspond to the cation distribution $^{VIII}\{Mn_{0\cdot88}\}$-$^{IV}[Pt]^{VI}(Pt_{1\cdot87}Mn_{0\cdot13})O_6$, and occupancy values in Table 2 are given in atoms per formula unit in each Wyckoff position. Crystal-chemical implications of these eight-coordinated vacancies and details of the $MnPt_3O_6$ structure as deduced from the positional and unit-cell parameters are discussed below.

3.2. *Structure refinement of* $CoPt_3O_6$

The neutron powder diffraction data collected for $CoPt_3O_6$ at 2·46 Å were also fully indexed on a C-centered orthorhombic unit cell. However, a problem with the peak shapes of reflections with $l \neq 0$ eliminated the possibility of performing structure refinements with these data using the technique of profile analysis. This is illustrated for the 002 peak in Fig. 2, which is strongly asymmetric, and clearly cannot be fit to a Gaussian line shape. This is most likely due to intercrystalline stacking disorders along the c axis, *i.e.* a variability in the unit-cell parameter c from grain to grain in the powder sample.

Since the data are unsuitable for structure refinements by profile analysis, the program *POWLS* (Will, 1979) was used. This program, in which integrated intensities based upon stepwise summation of the raw data with a background correction are used, has previously been used successfully for refinement of the structure of $Co_{0\cdot37}Na_{0\cdot14}Pt_2O_4$, where diffuse ordering peaks were inadequately fit by *PROFILE* (Schwartz, Parise, Prewitt & Shannon, 1982). Small degrees of broadening of the 002 reflection were also seen in the neutron powder diffraction patterns for $ZnPt_3O_6$, $MgPt_3O_6$, and $NiPt_3O_6$, and *POWLS* was also used to refine these structures.

The results of the structure refinement for $CoPt_3O_6$ are given in column (II) of Table 2.* The data included 23 independent observations representing 35 reflections. Overlapping reflections which could not be resolved are summed and counted as a single observation. The refined parameters were a scale factor, one O(1) and two O(2) positional parameters, an overall temperature factor, and one occupancy parameter in the final stages of refinement.

The structure refinement was carried out in the same way as described for $MnPt_3O_6$, and the initial refinement assuming chemical stoichiometry yielded a weighted discrepancy factor $R_w = 0\cdot062$, with $\chi^2 = 1\cdot53$. Refinements of the various site scattering lengths showed eightfold vacancies and a Pt deficiency on the sixfold site indicative of Co disorder. The total Co content obtained from chemical analysis was then used to construct a general formula:

$$^{VIII}\{Co_{1\cdot32y-1\cdot53}\square_{2\cdot53-1\cdot32y}\}^{IV}[Pt]^{VI}(Pt_yCo_{2-y})O_6$$

with y the one additional variable parameter that determined the final cation distribution. This final refinement resulted in a decrease in the weighted discrepancy factor to $R_w = 0\cdot041$, with $\chi^2 = 1\cdot01$, and $R = 0\cdot025$. The final cation distribution deduced from this occupancy parameter was

$$^{VIII}\{Co_{0\cdot92}\}^{IV}[Pt]^{VI}(Pt_{1\cdot86}Co_{0\cdot14})O_6.$$

* See deposition footnote.

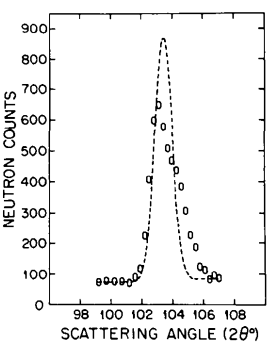

Fig. 2. Neutron powder diffraction profile of the 002 reflection for $CoPt_3O_6$ and an attempt by *PROFILE* to fit it to a Gaussian line shape.

3.3. *Structure refinements of* $ZnPt_3O_6$ *and* $MgPt_3O_6$

The results of refinements of the structures of $ZnPt_3O_6$ and $MgPt_3O_6$ in space group *Cmmm* are reported in columns (III) and (IV) of Table 2,* respectively. The data for $ZnPt_3O_6$ included 15 observations representing 26 reflections, and the data for $MgPt_3O_6$ included 25 observations representing 40 reflections. The diffraction peaks for $ZnPt_3O_6$ were broader than those for other samples, and some reflections which were possible to resolve in other samples had to be combined in this case (*e.g.* 130 + 220; 111 + 021; 241 + 420 and 060 + 331 + 151).

In contrast to the Mn and Co compounds, chemical analysis for Zn in $ZnPt_3O_6$ showed a slight cation deficiency, with 0·95 cations per formula unit based on stoichiometric amounts of Pt and O. In this case, occupancy refinements of the octahedral and planar sites showed no significant Pt deficiency. Structure refinement was therefore performed with the formula $^{VIII}\{Zn_{0.95}\}^{IV}[Pt]^{VI}(Pt_2)O_6$, and resulted in a weighted discrepancy factor of $R_w = 0.046$, with $\chi^2 = 1.44$.

The chemical analysis for Mg in $MgPt_3O_6$ also suggested a counterion deficiency, but the results were not reproducible to the same degree of precision as the other analyses and could have been affected by β-PtO_2 which was present in both X-ray and neutron powder diffraction patterns. The compound was therefore assumed to be stoichiometric $^{VIII}\{Mg\}^{IV}[Pt]^{VI}(Pt_2)O_6$, and no attempt was made to refine occupancy parameters. The final discrepancy factors $R = 0.053$, $R_w = 0.076$, and $\chi^2 = 2.07$ are significantly higher than for the previous refinements. In general, the poorest agreement was for reflections with $l \neq 0$, with a very bad fit for the 002 reflection. It is felt that this could be attributed to some degree of preferred orientation, with the needle-like crystals, elongated parallel to the *c* axis, oriented perpendicular to the axis of the cylindrically shaped pellet. This type of preferred orientation, unlike that from plate-like crystallites, could not be quantitatively modeled. It should enhance reflections with $l \neq 0$, and $I_{obs} > I_{calc}$ for reflections 001, 111, 021, and 002, with Δ/σ ranging from 2·0 to 4·0 for these reflections ($\Delta = I_{obs} - I_{calc}$; σ = estimated standard deviation of the observed intensity). However, the refined positional parameters are not a function of the intensities of 001 or 002, and are thus not greatly affected by the problem of preferred orientation.

The overall temperature factors for these two structure refinements are both negative, but by one standard deviation or less. It is not obvious why this should be so, though for $MgPt_3O_6$ it may be an artifact to compensate for the discrepancy between observed and calculated intensities for reflections with $l \neq 0$. In any case, the thermal parameters are not correlated with the O positional parameters, the correlation coefficients being $<|20|$ in all cases, so the presence of slightly negative temperature factors does not cast doubt on the refined values of the O positions.

* See deposition footnote.

3.4. *Structure refinement of* $NiPt_3O_6$

The neutron powder diffraction pattern for $NiPt_3O_6$ could also be indexed on an orthorhombic unit cell, but there were reflections which violated the absence rule for *C*-centered lattices. This change in symmetry implied significant internal distortion of the *Cmmm* MPt_3O_6 structure accompanying the presence of Ni. Examination of X-ray and neutron powder diffraction patterns for $NiPt_3O_6$ indicated systematic absences of the type $0kl$: $k \neq 2n$ and $h0l$: $h \neq 2n$.

The results of the refinement of the $NiPt_3O_6$ structure in *Pbam* are given in Table 3,* along with site information for the atomic positions. The data included 28 observations including 64 independent reflections. The refined parameters were a scale factor, an *x* and *y* positional parameter for Pt(2) and three inequivalent O atoms, an overall temperature factor, and one occupancy parameter which modelled the distribution of Ni over the eight-coordinated and four-coordinated sites.

Chemical analysis for Ni in $NiPt_3O_6$ indicated a Ni content considerably in excess of 1·0 cations per formula unit. A preliminary refinement assuming chemical stoichiometry resulted in a weighted discrepancy factor $R_w = 0.060$, with $\chi^2 = 1.79$. Refinement of O occupancies assuming cation stoichiometry did not improve the discrepancy factors, and the O sites were presumed to be fully occupied. In contrast

* See deposition footnote.

Table 3. *Structure refinement for* $NiPt_3O_6$ *(orthorhombic, Pbam)*

		x	*y*	*z*
^{VIII}Ni	2(*c*)	½	0	0
^{IV}Pt(1)	2(*a*)	0	0	0
^{VI}Pt(2)	4(*h*)	*x*	*y*	½
O(1)	4(*h*)	*x*	*y*	½
O(2)	4(*g*)	*x*	*y*	0
O(3)	4(*g*)	*x*	*y*	0

Occupancy:* ^{VIII}Ni	1·00 (1)†	*x*: O(2)	0·227 (3)
Occupancy: ^{IV}Pt	0·86 (1)	*y*: O(2)	0·113 (1)
Occupancy: ^{IV}Ni	0·14 (1)	*x*: O(3)	0·311 (2)
Occupancy: ^{VI}Pt	2·0	*y*: O(3)	0·357 (1)
Occupancy: O	6·0	*B* (overall)‡	0·2 (2)
x: Pt(2)	0·233 (1)	χ^2	1·53
y: Pt(2)	0·259 (1)	*R*	0·035
x: O(1)	−0·018 (3)	R_w	0·050
y: O(1)	0·353 (1)		

* Occupancies given in atoms per formula unit (see text).
† Errors in parentheses.
‡ Overall isotropic temperature factor (Å²).

to $MnPt_3O_6$ and $CoPt_3O_6$, preliminary refinements of the site scattering lengths resulted in an excess of scattering power on the planar site, with the scattering length of the sixfold site consistent with stoichiometric Pt occupancy. Since the neutron scattering length for Ni is greater than that for Pt, this result indicated Ni disorder between the eightfold and planar fourfold sites. Ni is occasionally found to occur in planar coordination in oxides, so separate refinements were performed in which Ni was allowed to be distributed between the eight-coordinated, and either the six-coordinated or planar sites. As with the occupancy refinements described above for $MnPt_3O_6$ and $CoPt_3O_6$, the total Ni content was constrained to the chemically analyzed value and the Pt site containing some Ni (with either six- or fourfold coordination) was constrained to be fully occupied. The refinement in which Ni was assumed to be distributed between eight- and sixfold coordinated sites would not converge at all, while the refinement with Ni occupancy in planar coordination converged with final discrepancy factors $R_w = 0{\cdot}050$ and $R = 0{\cdot}035$, with $\chi^2 = 1{\cdot}53$. The general formula for the final refinement was:

$$^{VIII}\{Ni_{1{\cdot}34z-0{\cdot}15}\square_{1{\cdot}15-1{\cdot}34z}\}^{IV}[Pt_zNi_{1-z}]^{VI}(Pt_2)O_6.$$

All other refined parameters were within one standard deviation of the values obtained from the refinement assuming chemical stoichiometry. Hence, the addition of the refined parameter z led to a decrease in R_w from 0·060 to 0·050. The final cation distribution was $^{VIII}\{Ni\}^{IV}[Pt_{0{\cdot}86}Ni_{0{\cdot}14}]^{VI}(Pt_2)O_6$. A comparison of the *Pbam* $NiPt_3O_6$ structure with the *Cmmm* structure is given below.

4. The structure of orthorhombic MPt_3O_6 compounds

4.1. *Primary characteristics of the* MPt_3O_6 *structure*

The *C*-centered MPt_3O_6 structure of $CdPt_3O_6$ and M = Mn, Co, Zn, and Mg compositions studied here contains three types of cation coordination polyhedra. The structure is shown in Fig. 3(*a*) as a projection down the *c* axis, with a perspective view shown in Fig. 3(*b*). The ^{IV}Pt(1) site at 0,0,0 is surrounded by four O(2) atoms in planar coordination on a mirror plane perpendicular to the *c* axis. This planar site shares its two edges parallel to the *b* axis with the ^{VIII}M polyhedral site. The counterion site on this mirror plane, at $\frac{1}{2}$,0,0, is coordinated by four additional O(1) atoms at $z = \pm\frac{1}{2}$ to complete its eight-coordinated polyhedron. The ^{VI}Pt(2) site at $\frac{1}{4},\frac{1}{4},\frac{1}{2}$ is thus coordinated by four O(2) atoms in a planar arrangement and two O(1) atoms which form the vertices of a distorted octahedral site. This octahedral site can also contain counterion atoms.

The MPt_3O_6 structure can be described in terms of the PtO_4 groups arranged in stacks forming columns of ^{IV}Pt cations along [001] perpendicular to the plane of each site. The columnar stacks of PtO_4 groups are linked together in the xy plane by bridging MO_8 and octahedral coordination polyhedra. Since both MO_8 and PtO_6 polyhedra are edge-linked to equivalent polyhedra along [001], the resulting structure contains infinite columns of edge-linked MO_8 and PtO_6 polyhedra as well as columnar stacks of PtO_4 groups, with each column containing metal–metal distances of $<3{\cdot}15$ Å. This unique structural feature has implications for the chemistry and physical properties of MPt_3O_6 compounds.

The *C*-centered MPt_3O_6 compounds examined in this study all contain counterions 0·15–0·21 Å smaller than the prototype counterion, Cd. In cubic MPt_3O_4 compounds, which contain columnar stacks of PtO_4 groups parallel to all three crystallographic axes (Schwartz, Parise, Prewitt & Shannon, 1982), small counterions do not change the structure to the degree expected based on ionic-radii considerations. This is due to the rigid nature of the PtO_4 groups. Bond distances and angles for *C*-centered MPt_3O_6 structures, including $CdPt_3O_6$ (Prewitt, Schwartz &

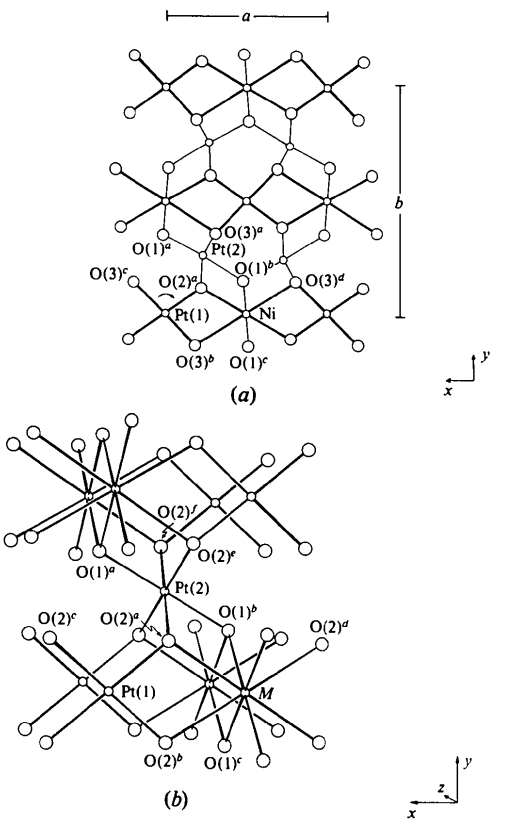

Fig. 3. *ORTEP* (Johnson, 1965) drawings of the *C*-centered MPt_3O_6 structure projected (*a*) down [001] (atoms in the asymmetric unit cell are labeled), and (*b*) sub-parallel to the *c* axis.

Table 4. *Bond distances* (Å) *and angles* (°)

(*a*) MPt_3O_6 (*Cmmm*)

	Mn	Co	Zn	Mg	Cd*
Ionic radii†	0·96	0·90	0·90	0·89	1·10
4‡ ^{IV}Pt–O(2)	1·98 (1)	1·97 (1)	1·94 (1)	1·95 (1)	1·99 (1)
2 ^{VI}Pt–O(1)	2·02 (<1)	2·03 (<1)	2·03 (1)	2·03 (1)	2·01 (1)
4 ^{VI}Pt–O(2)	2·02 (1)	2·00 (1)	2·03 (1)	2·02 (1)	2·03 (1)
4 ^{VIII}M–O(1)	2·22 (1)	2·17 (1)	2·19 (1)	2·18 (1)	2·29 (1)
4 ^{VIII}M–O(2)	2·44 (1)	2·40 (1)	2·40 (1)	2·42 (1)	2·48 (1)
Pt(1)–O(2) rectangle					
$O(2)^a$–$O(2)^c$	3·00 (1)	3·00 (1)	3·01 (1)	2·99 (1)	3·00 (1)
$O(2)^a$–$O(2)^b$	2·57 (2)	2·54 (2)	2·45 (2)	2·51 (2)	2·63 (2)
$O(2)^a$–Pt–$O(2)^b$	81·1 (5)	80·5 (5)	78·3 (6)	79·9 (5)	82·4 (5)
$Pt(2)O_6$ octahedron					
$O(2)^a$–$O(2)^e$	2·52 (2)	2·48 (2)	2·59 (2)	2·53 (2)	2·54 (2)
$O(2)^e$–$O(2)^f$	3·148 (<1)	3·143 (1)	3·138 (1)	3·141 (1)	3·165 (<1)
$O(1)^a$–$O(2)^f$	2·62 (1)	2·59 (1)	2·61 (1)	2·61 (1)	2·66 (1)
$O(2)^e$–$O(2)^b$	3·07 (1)	3·09 (1)	3·11 (1)	3·09 (1)	3·04 (1)
$O(2)^a$–Pt–$O(2)^e$	77·3 (4)	76·7 (5)	79·0 (4)	77·7 (4)	77·5 (5)
$O(1)^a$–Pt–$O(2)^e$	80·9 (3)	79·8 (2)	79·9 (3)	80·3 (4)	82·3 (4)
M–O(1) rectangle					
$O(1)^b$–$O(1)^c$	3·13 (2)	3·00 (2)	3·05 (4)	3·02 (4)	3·32 (4)
$O(1)^b$–*M*–$O(1)^c$	89·8 (4)	87·4 (4)	88·3 (8)	87·8 (8)	92·7 (7)
M–O(2) rectangle					
$O(2)^a$–$O(2)^d$	4·15 (1)	4·09 (1)	4·12 (1)	4·13 (1)	4·21 (1)
$O(2)^a$–*M*–$O(2)^b$	63·6 (4)	63·9 (5)	61·4 (4)	62·5 (5)	63·9 (5)

* Based on single-crystal X-ray diffraction structure refinement (Prewitt, Schwartz & Shannon, 1983).
† Ionic radii in Å for divalent species in eight-coordination (Shannon, 1976).
‡ Multiplicity of bonds in the coordination polyhedron.

Table 4 (*cont.*)

(*b*) $NiPt_3O_6$ (*Pbam*)

2 ^{IV}Pt–O(2)	1·97 (2)	1 ^{VI}Pt–$O(1)^a$	2·02 (2)
2 ^{IV}Pt–O(3)	1·96 (1)	1 ^{VI}Pt–$O(1)^b$	2·09 (2)
4 ^{VIII}Ni–O(1)	2·13 (1)	2 ^{VI}Pt–O(2)	2·12 (1)
2 ^{VIII}Ni–O(2)	2·25 (2)	2 ^{VI}Pt–O(3)	1·91 (1)
2 ^{VIII}Ni–O(3)	2·63 (1)		
Pt(1)–O(2,3) parallelogram			
$O(2)^a$–$O(3)^c$	2·98 (1)	$O(2)^a$–Pt–$O(3)^b$	81·3 (4)
$O(2)^a$–$O(3)^b$	2·56 (1)	$O(3)^b$–$O(2)^a$–$O(3)^c$	89·7 (7)
$Pt(2)O_6$ octahedron			
$O(2)^a$–$O(2)^b$	3·100 (1)	$O(1)^a$–Pt–$O(1)^b$	175·5 (8)
$O(2)^a$–$O(3)^a$	2·50 (1)	$O(1)^a$–Pt–$O(2)^a$	107·4 (5)
$O(1)^a$–$O(3)^a$	2·81 (3)	$O(1)^a$–Pt–$O(3)^a$	91·3 (6)
$O(1)^a$–$O(2)^a$	3·36 (3)	$O(1)^b$–Pt–$O(2)^a$	69·8 (7)
$O(2)^a$–$O(1)^b$	2·41 (3)	$O(1)^b$–Pt–$O(3)^a$	91·4 (4)
$O(3)^a$–$O(1)^b$	2·87 (1)	$O(2)^a$–Pt–$O(2)^b$	93·8 (4)
		$O(2)^a$–Pt–$O(3)^a$	76·2 (3)
		$O(2)^a$–Pt–$O(3)^e$	160·9 (8)
		$O(3)^a$–Pt–$O(3)^e$	108·3 (4)
M–O(1) rectangle			
$O(1)^b$–$O(1)^c$	2·93 (2)	$O(1)^b$–Ni–$O(1)^c$	86·8 (4)
M–O(2,3) parallelogram			
$O(2)^a$–$O(3)^d$	4·17 (1)	$O(2)^a$–Ni–$O(3)^b$	62·7 (3)
		$O(3)^b$–$O(2)^a$–$O(3)^d$	100 (1)

Shannon, 1983), in Table 4(*a*), again demonstrate this point. The structural differences amongst the various MPt_3O_6 compositions are small, considering the range in ionic radii of the various counterions present. However, the presence of ^{VIII}Ni is accompanied by the loss of *C*-centered symmetry. A comparison of the *C*-centered and primitive MPt_3O_6 structures is given below.

4.2. *C-Centered and primitive* MPt_3O_6: *distortions of the cation coordination polyhedra with a* Ni *counterion*

Figs. 4(*a*) and 4(*b*) demonstrate the similarities of primitive MPt_3O_6 and *C*-centered MPt_3O_6. The columns of PtO_4, PtO_6, and MO_8 polyhedra along the *c* axis remain intact. The unit-cell dimensions of $NiPt_3O_6$ are comparable with those of $CoPt_3O_6$, $ZnPt_3O_6$, and $MgPt_3O_6$, though there is a decrease in the *c* dimension of over 0·04 Å. The $NiPt_3O_6$ structure is the only known oxide with Ni in eight-coordination as a stoichiometric component. The bond distances and angles are given in Table 4(*b*).

A major difference between *C*-centered and primitive MPt_3O_6 is the loss of symmetrical equivalence of adjacent O atoms on the mirror plane at $z = 0$. Whereas in *C*-centered MPt_3O_6 all four O atoms of the PtO_4 planar site are equivalent O(2) atoms, in $NiPt_3O_6$ there are two sets of O atoms, O(2) and O(3), with each pair related by a center of symmetry on which the Pt(1) atom resides. In *C*-centered MPt_3O_6, the planar PtO_4 group is a rectangle with four equivalent Pt–O(2) bond distances. In primitive $NiPt_3O_6$, the PtO_4 polyhedron (which contains 14% ^{IV}Ni) is reduced in symmetry to a parallelogram. The angular distortion of the planar

group is very small and the Pt—O(2) bond distances are virtually equal to the Pt—O(3) distances. However, though the PtO_4 groups are unchanged in their internal dimensions, they are rotated with respect to the *a* and *b* axes by 6°, with $O(2)^a$ moving towards the Ni at $-\frac{1}{2},0,0$ and $O(3)^b$ moving away (Fig. 4*a*). This is yet another demonstration of the rigidity of PtO_4 planar groups which are a fundamental structural unit of MPt_3O_4 and MPt_3O_6 compounds.

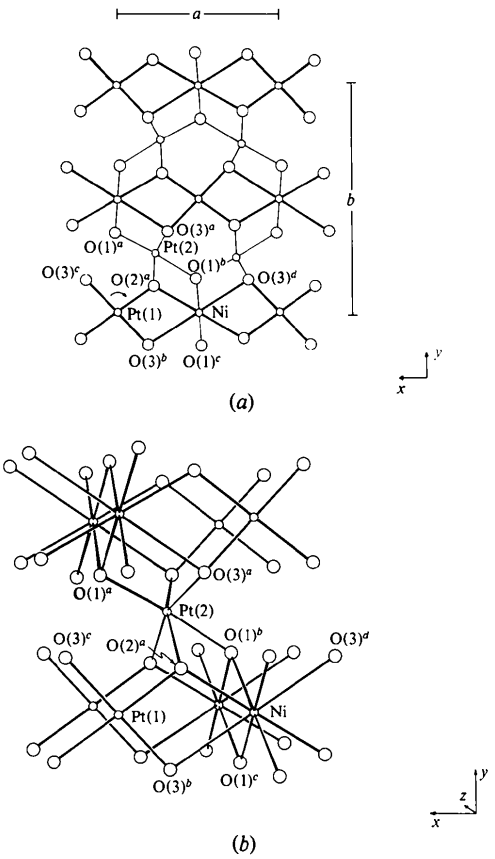

Fig. 4. *ORTEP* drawings of the primitive $NiPt_3O_6$ structure projected (*a*) down [001] (the arrow indicates rotation of planar site), and (*b*) sub-parallel to the *c* axis.

Metal—oxygen bond distances in the six-coordinated site of the *C*-centered MPt_3O_6 structure are virtually equal and unchanged for all compositions studied. The octahedral site is orthorhombically distorted, with the Pt cation on an inversion center having point symmetry 2/*m*. This center of symmetry is lost in the primitive $NiPt_3O_6$ structure, and the six-coordinated site has Pt—O distances from 1·91 (1) to 2·12 (1) Å (Fig. 5). The Pt cation is no longer coplanar with four O atoms and no longer collinear with its two coordinating O(1) atoms. The mean dimensions and distortions of the octahedral coordination polyhedron for all compositions studied are given in Table 5. The average ^{VI}M—O and O—O distances are within the range of previously studied PtO_6 octahedra containing tetravalent Pt (Wellmann & Liebau, 1981 and reference within). In terms of angular dimensions, the MPt_3O_6 structure, and particularly $NiPt_3O_6$, contains a highly distorted octahedral site.

The eight-coordinated counterion site shows the most variation in metal—oxygen distances with changing counterions for the *C*-centered structure. The variation is qualitatively consistent with ionic-radii considerations, with four *M*—O(1) and four *M*—O(2) distances for Cd > Mn > Co ≃ Zn ≃ Mg. The eightfold site consists of two intersecting rectangular planes: an O(1) plane perpendicular to the *a* axis and an O(2)

Table 5. *Dimensions and distortions in* $[PtO_6]$ *octahedra for* MPt_3O_6

$\Delta Pt{-}O = (Pt{-}O)_{max} - (Pt{-}O)_{min}$.
$\Delta(O{-}Pt{-}O) = |(O{-}Pt{-}O) - 90|_{max}$.

	Mean values		Distortions	
	Pt—O	O—O	Δ(Pt—O)	Δ(O—Pt—O)
$MnPt_3O_6$	2·02 Å	2·84 Å	0·0 Å	12·7°
$CoPt_3O_6$	2·01	2·83	0·03	13·3
$ZnPt_3O_6$	2·03	2·86	0·0	11·0
$MgPt_3O_6$	2·02	2·85	0·01	12·3
$CdPt_3O_6$*	2·02	2·85	0·02	13
$NiPt_3O_6$	2·03	2·84	0·21	20·2

* Based on single-crystal X-ray diffraction structure refinement (Prewitt, Schwartz & Shannon, 1983).

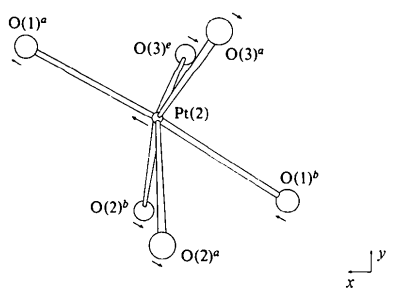

Fig. 5. *ORTEP* drawing of the distorted six-coordinated Pt(2) coordination polyhedron in primitive $NiPt_3O_6$. Arrows indicate O movement relative to the ideal *C*-centered structure.

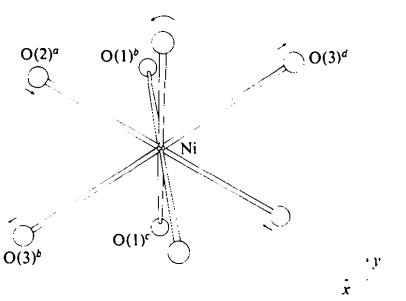

Fig. 6. *ORTEP* drawing of the distorted eight-coordinated counterion coordination polyhedron in primitive $NiPt_3O_6$. Arrows indicate O movement relative to the ideal *C*-centered structure.

plane perpendicular to the c axis. For primitive $NiPt_3O_6$, the O(2) rectangle is distorted to an O(2)–O(3) parallelogram, as the rotation of the PtO_4 groups mentioned above shifts O(2) atoms towards Ni and O(3) atoms away (Fig. 6). The O(1) rectangle remains intact, but rotates out of the bc plane about the twofold axis by 5°.

5. Discussion

The small degree of structural change in C-centered MPt_3O_6 with changing counterion size is another example of the rigidity of the structures of complex platinum oxides. As in $Li_{0.64}Pt_3O_4$ and $Co_{0.37}Na_{0.14}Pt_3O_4$ (Schwartz, Parise, Prewitt & Shannon, 1982), the Pt—O distances vary very little, and structural compensation for the substitution of small eight-coordinated counterions by shortening of the M—O bond distances is not comparable to the reduction in counterion size relative to the ideal counterion, *i.e.* Cd for MPt_3O_6 or Na for MPt_3O_4. Angular distortions of Pt coordination polyhedra, however, are observed.

Many of the changes in the MPt_3O_6 structure are reflected in the unit-cell parameters. These changes can be related to changes in O—O distances of the two intersecting planes which compose the MO_8 coordination polyhedron. For example, the shortened unit-cell parameter a for $CoPt_3O_6$ is related to the $O(2)^a$–$O(2)^d$ distance and the unit-cell parameter b is related to the $O(1)^b$–$O(1)^c$ distance. These changes are due more to angular distortions of the M—O(1) and M—O(2) rectangular planes than to changes in the M—O bond distances, especially when comparing differences in unit-cell parameters for MPt_3O_6 structures with counterions of the same size.

The eight-coordinated counterion site of MPt_3O_6 is itself notable for two reasons: its symmetry and some of the cations which occupy it. Though cubic eight-coordination is seen in ionic solids such as CsCl and CaF_2, and in MPt_3O_4 compounds (Schwartz, Parise, Prewitt & Shannon, 1982), where O atoms form continuous arrays, the coordination chemistry for eight-coordinated metals is dominated by a set of low-energy geometries including the square (Archimedean) antiprism and the triangulated dodecahedron (bisdisphenoid) (Hoard & Silverton, 1963; Burdett, Hoffmann & Fay, 1978 and references within). Both these polyhedra, having D_{4d} ($\bar{8}2m$) and D_{2d} ($\bar{4}2m$) symmetry, respectively, can be derived from distortions of a cube, as shown in Fig. 7. These two coordination polyhedra are the most energetically stable with respect to ligand–ligand repulsions (Hoard & Silverton, 1963; Kepert, 1965). The eight-coordinated counterion site in the C-centered MPt_3O_6 structure is an orthorhombically distorted cube with D_{2h} (mmm) symmetry (Fig. 7c). This type of coordination polyhedron does not have an energetically favorable arrangement of ligands but, as was also seen in the MPt_3O_4 structure (Schwartz, Parise, Prewitt & Shannon, 1982), the rigid PtO_4 planar groups prevent a more favorable O configuration.

Eight-coordination is not common for late-group first-row transition metals containing more than two d electrons, but there are examples for Co^{2+}, Mn^{2+}, and Zn^{2+} which were cited earlier (see also Burdett, Hoffmann & Fay, 1978). Eight-coordination has not previously been reported for Ni^{2+}. These examples of eight-coordination for late-group transition metals are for dodecahedral configurations, the common polyhedron for these species. In the C-centered MPt_3O_6 structure, these same transition metals are in an eight-coordinated site consisting of two intersecting O rectangles coinciding with mirror planes perpendicular to the a axis and the c axis. The only similar type of coordination polyhedron has been reported for Mn^{3+} and Cu^{2+} in the isostructural compounds $NaMn_7O_{12}$ and $CaCu_3Mn_4O_{12}$ (Marezio, Dernier, Chenavas & Joubert, 1973; Chenavas, Joubert, Marezio & Bochu, 1975). The prototype $NaMn_7O_{12}$ has a distorted perovskite structure, with Mn^{3+} cations occupying a highly distorted A site [symmetry D_{2h} (mmm)] surrounded by three orthogonal sets of O rectangular planes comprising a 12-O-atom polyhedron. The three sets of Mn^{3+}—O distances are 1·91, 2·69, and 3·26 Å, and the third set of four O atoms is characterized as second-nearest neighbors. The Mn^{3+} (and Cu^{2+} in $CaCu_3Mn_4O_{12}$) coordination number is therefore described as 4 + 4.

The loss of C-centered symmetry for the primitive $NiPt_3O_6$ structure indicates the unusual nature of eight-coordinated Ni as compared with other eight-coordinated first-row transition metals. Divalent Ni, with eight d electrons, is a well known Jahn–Teller

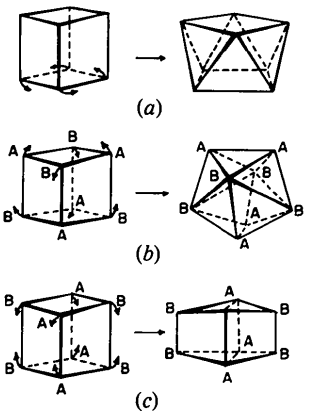

Fig. 7. Distortions of a cubic (O_h) eight-coordinated site. (a) Archimedean square antiprism (D_{4d}). (b) Triangulated dodecahedron (D_{2d}). (c) Orthorhombic distortion seen in C-centered MPt_3O_6 structures (D_{2h}) (after Hoard & Silverton, 1963; Cotton & Wilkinson, 1966).

cation. Examination of the O movement about the Ni^{2+} cation (Fig. 6) shows that the eight-coordinated site is distorting towards an octahedral configuration, which would result in a more energetically favorable electron configuration for a d^8 transition metal. A combination of the small size of Ni and the Jahn–Teller effect could explain the highly distorted nature of the counterion site, and the $NiPt_3O_6$ structure as a whole.

The results of magnetic-susceptibility measurements on the $MnPt_3O_6$, $CoPt_3O_6$, and $NiPt_3O_6$ compositions studied here are consistent with a divalent state for eight-coordinated counterions (Schwartz & Parise, 1982). Therefore, counterion disorder in $^{VIII}\{Mn_{0.88}\square_{0.12}\}^{IV}[Pt]^{VI}(Pt_{1.87}Mn_{0.13})O_6$ and $^{VIII}\{Co_{0.92}\square_{0.08}\}^{IV}[Pt]^{VI}(Pt_{1.86}Co_{0.14})O_6$ must be accompanied by a non-integral oxidation state for Pt. Chemical non-stoichiometry in materials containing columnar stacks of PtO_4 groups suggests the possibility for partial oxidation of the Pt^{2+} chains and mixed-valence electronic interactions. Partially oxidized columnar stacks of PtO_4 groups in $Na_xPt_3O_4$ have already been associated with chemical non-stoichiometry, delocalized electrons, and metallic conductivity (*e.g.* Schwartz, Prewitt, Shannon, Corliss, Hastings & Chamberland, 1982). Room-temperature electrical conductivities measured on single crystals of $CoPt_3O_6$ and $Mn_{1+x}Pt_{3-x}O_6$ ($x \sim 0{\cdot}2$) are 4×10^3 and $1 - 2 \times 10^4\ \Omega^{-1}\ m^{-1}$, respectively, with activation energies $E_a < 0{\cdot}1$ eV (Schwartz, Gillson & Shannon, 1982). This demonstrates that these are highly conducting semiconductors containing significant metal–metal interactions.

The structures of MPt_3O_6 compounds are anisotropic, with columnar stacks of PtO_4 groups and chains of edge-linked polyhedra containing octahedrally or eight-coordinated metals extending along [001]. This is consistent with evidence that one-dimensional (1D) electronic interactions occur in MPt_3O_6 (M = Mn, Co) (Schwartz & Parise, 1982). Low-dimensional electronic interactions result in unique physical properties, such as 1D electrical conductivity. Other examples of 1D conductors containing partially oxidized columnar stacks of four-coordinated planar Pt include the well known partially oxidized tetracyanoplatinates, *e.g.* $K_2Pt(CN)_4Br_{0.30}.3H_2O$ (see Williams & Schultz, 1979, for example). The MPt_3O_6 structure, with its ability to accommodate variations in counterion composition and concentration and its high thermal stability (to 923–973 K) (Hoekstra, Siegel & Gallagher, 1971) relative to other 1D conductors, provides an opportunity for further study of the relationships of structure, crystal chemistry, and electronic interactions in anisotropic materials at ambient conditions and at elevated temperatures and pressures.

We would like to thank D. E. Cox for experimental and interpretive assistance throughout this entire project, L. M. Corliss and J. M. Hastings for neutron powder diffraction data collection at $\lambda = 1{\cdot}34$ Å, C. M. Foris for Guinier XRD photographs, R. J. Burnett and F. C. Diffendall for operation of the internally heated reactor, and B. F. Burgess and C. R. Perrotto for atomic absorption analyses. The work was performed under NSF Grant DMR79-06900 and at the Experimental Station of E.I. du Pont de Nemours and Company.

References

BACON, G. E. (1978). Brookhaven National Laboratory compilation (unpublished).

BELLITO, C., GASTALDI, L. & TOMLINSON, A. A. G. (1976). *J. Chem. Soc. Dalton Trans.* pp. 989–992.

BERGMAN, J. G. & COTTON, F. A. (1966). *Inorg. Chem.* **5**, 1208–1213.

BURDETT, J. K., HOFFMANN, R. & FAY, R. C. (1978). *Inorg. Chem.* **17**, 2553–2568.

CAHEN, D., IBERS, J. A. & WAGNER, J. B. (1974). *Inorg. Chem.* **13**, 1377–1388.

CARCIA, P. F., SHANNON, R. D. & STAIKOS, D. N. (1981). US patent 4 264 685.

CHENAVAS, J., JOUBERT, J. C., MAREZIO, M. & BOCHU, B. (1975). *J. Solid State Chem.* **14**, 25–32.

COTTON, F. A. & WILKINSON, G. (1966). *Advanced Inorganic Chemistry*, 2nd ed. New York: Interscience.

HEWAT, A. E. (1973). UK Atomic Energy Authority Research Group Report RLL 73/897 (unpublished).

HOARD, J. L. & SILVERTON, J. V. (1963). *Inorg. Chem*, **2**, 235–243.

HOEKSTRA, H. R., SIEGEL, S. & GALLAGHER, F. X. (1971). *Adv. Chem. Ser.* No. 98, pp. 39–53.

JOHNSON, C. K. (1965). *ORTEP*. Report ORNL-3794. Oak Ridge National Laboratory, Tennessee.

KEPERT, D. L. (1965). *J. Chem. Soc.* pp. 4736–4744.

KOESTER, L. (1977). *Springer Tracts Mod. Phys.* **80**, 1–55.

MAREZIO, M., DERNIER, P. D., CHENAVAS, J. & JOUBERT, J. C. (1973). *J. Solid State Chem.* **6**, 16–20.

MULLER, O. & ROY, R. (1969). *J. Less-Common Met.* **19**, 209–214.

PREWITT, C. T., SCHWARTZ, K. B. & SHANNON, R. D. (1983). *Acta Cryst.* C**39**. To be published.

RIETVELD, H. M. (1969*a*). Reactor Centrum Nederland Research Report RCN 104 (unpublished).

RIETVELD, H. M. (1969*b*). *J. Appl. Cryst.* **2**, 65–71.

SCHWARTZ, K. B., GILLSON, J. L. & SHANNON, R. D. (1982). *J. Cryst. Growth*. In the press.

SCHWARTZ, K. B. & PARISE, J. B. (1982). *J. Phys. Chem. Solids*, **43**, 911–917.

SCHWARTZ, K. B., PARISE, J. B., PREWITT, C. T. & SHANNON, R. D. (1982). *Acta Cryst.* B**38**, 2109–2116.

SCHWARTZ, K. B., PREWITT, C. T., SHANNON, R. D., CORLISS, L. M., HASTINGS, J. M. & CHAMBERLAND, B. L. (1982). *Acta Cryst.* B**38**, 363–368.

SHANNON, R. D. (1972). US patent 3 663 181.

SHANNON, R. D. (1976). *Acta Cryst.* A**32**, 751–767.

WELLMANN, B. & LIEBAU, F. (1981). *J. Less-Common Met.* **77**, P31–P39.

WILL, G. (1979). *J. Appl. Cryst.* **12**, 483–485.

WILLIAMS, J. M. & SCHULTZ, A. J. (1979). *Molecular Metals*. NATO Conf. Ser. VI, Vol. 1, edited by W. E. HATFIELD, pp. 337–368. New York: Plenum.